A&A 434, 221–233 (2005)
DOI: 10.1051/0004-6361:20041466

Astronomy & Astrophysics

H_α observations of the star FK Com⋆

D. P. Kjurkchieva and D. V. Marchev

Department of Physics, Shoumen University, 9700 Shoumen, Bulgaria
e-mail: [d.kyurkchieva;d.marchev]@shu-bg.net

Received 14 June 2004 / Accepted 9 December 2004

Abstract. High-resolution spectroscopic observations around the H_α line of FK Com are presented. The analysis of the spectra reveals that: (a) the intensity of the *R* peak of the mean H_α profile is larger than that of the *V* peak; (b) the intensities of the *V* and *R* emission peaks changes almost in anti-phase; (c) the ratio V/R varies in phase with *V*; (d) the total H_α emission has a maximum at phase 0.75. The similarity of the H_α profile of FK Com with those of the disk-like stars leads us to the conclusion that its broad two-peaked emission H_α line originates from an extended disk. It is supposed that the disk produces the mean H_α line. The variability of the H_α profile is explained by the presence of additional sources of absorption and emission at diametrically opposite regions of the disk. The asymmetry of the mean H_α profile requires the disk to be half-illuminated. It is supposed that a source of illumination is a low-mass hot secondary orbiting the disk. A model of the H_α emitting configuration of FK Com is proposed.

Key words. stars: activity – stars: binaries: spectroscopic – stars: chromospheres – stars: individual: FK Com

1. Introduction

FK Com has been recognized as peculiar since Merrill (1948) who found it to be a G giant with broad absorption spectral lines. Later emission features have been discovered at CaII H and K and at H_α lines (Bidelman 1954; Herbig 1958). The star was found to be photometrically variable (Chugainov 1966; Rucinski 1981) with a period 2.4 days and amplitude of 0.07−0.14 mag increasing with decreasing wavelength (Morris & Milone 1983). Dorren et al. (1984) found that the light curve is rapidly changing in amplitude, shape and phase of light minimum but the photometric period appears constant over decades.

Rucinski (1981) established that the *UBVRI* colors of FK Com are not consistent with any normal star and explained $V-R$ and $R-I$ excesses by emission from circumstellar material. Bopp (1982) did not confirm presence of infrared excess and found that the 2−10 μm energy distribution of the star is characteristic of a giant.

Ramsey et al. (1981) and Walter & Basri (1982) detected very broad H_α emission lines with a strongly variable profile that is unusual in late-type stars. Welty & Ramsey (1994a) found that the H_α variations have the same period as the light variability. All the Balmer lines of FK Com show excess emission though only H_α has emission above the continuum. The strengths of CaII lines are modulated in phase with H_α but have not velocity-modulated wings like H_α (Huenemoerder et al. 1993).

FK Com shows strong chromospheric and transition region emission lines in the ultraviolet, revealing that its atmosphere is more extended than those of normal giant. The fluxes of the UV lines are larger than in other stars of similar spectral type and vary with photometric phase. The MgII h and k lines are in emission with sharp deep central absorption features. The flux densities in the CaII and the MgII lines exceed those expected from the main activity-rotation relation. Bopp & Stencel (1981) as well as Bianchi & Grewing (1987) conclude that FK Com has extremely active chromospheric and transition regions reaching the "saturation" limit in the period-activity relation of magnetically active dynamo-stars. The phase relation between the light curve and the intensities of the emission UV lines is opposite to that of the RS CVn stars (Bianchi et al. 1985).

X-ray emission from this star is also detected (Walter 1981; Welty & Ramsey 1994b). The X-ray observations of Gondoin et al. (2002) reveal that the corona of FK Com is dominated by large magnetic structures similar in size to interconnecting loops between solar active regions but significantly hotter. The ratio L_x/L_{bol} of FK Com is quite lower than that of the RS CVn star AR Lac near the same period (White et al. 1987; Bopp & Stencel 1981). So, in absolute terms FK Com is several times brighter in the chromosphere than RS CVn systems and only half as bright in the corona.

The radio luminosity of FK Com is similar to those of active cool stars (Hughes & McLean 1987; Rucinski 1991). The model of its radio spectrum with a thermal source leads to an inordinately large radius of 115 $R_\odot$ and the radio emission is attributed to acceleration of electrons in coronal streamers

⋆ Based on spectral observations collected at the National Astronomical Observatory at Rozhen.

controlled by the magnetic field of underlying star spots. The emission of FK Com at 3.6 cm show flare activity and rotational modulation with the maximum of the radio flux coinciding with the optical light maximum (Rucinski 1991).

Thus the activity of the star is well documented at all wavelengths, from X-rays to the radio domain. The level of the activity varies significantly within short periods of time (Jetsu et al. 1994). The phases of the photometric minima reveal that the active regions of FK Com show a "flip-flop" effect (Jetsu et al. 1991, 1993) that is discussed in the framework of nonlinear mean-field dynamo theory (Tuominen et al. 2002).

The chronology of the H_α flares implies that the H_α activity is triggered by activity close to the stellar surface and is interpreted by ejection of two cool shells (the second one with a bigger velocity) that later collide and shock (Dorren et al. 1984). Oliveira & Foing (1999) detected in FK Com the largest H_α flare reported on a cool star.

The approximately estimates for the distance and mass of FK Com as a member of the HR 1614 old disk aggregate are: d = 200−300 pc and $M = 1.5\ M_\odot$ (Guinan & Robinson 1986; Eggen & Iben 1989).

Firstly FK Com is considered as an RS CVn system (Bolton 1978) due to the similarity of its photometric and spectral properties to those observed in RS CVn and BY Dra stars (Hall 1976; Bopp & Evans 1973). However FK Com shows two characteristics not seen in RS CVn-type stars: (a) lack of an observable radial velocity variation due to a binary nature (McCarthy & Ramsey 1984; Huenemoerder et al. 1993); (b) broad H_α emission line with a strongly variable profile. Due to these characteristics Bopp & Rucinski (1981) suggest that FK Com defines a class of single, rapidly rotating giant stars. Later a few other stars were discovered with characteristics similar to those of FK Com: fast rotating G−K giants; strong chromospheric and transition region emission; light variability with amplitude of 0.1−0.2 mag; photometric periods of a few days (Carniero 1990; Cutispoto et al. 1992; Jetsu et al. 1992). But so far there is not a general agreement about the configurations of the FK Com-type stars.

It is impossible to infer the configuration of FK Com (single or double star) from photometric observations due to the small amplitude of its light variations and their irregularity. The goal of our prolonged spectral observations of FK Com was to study the behavior of its H_α line and to determine the sources of its emission. This information could help to learn more about the configuration of this star.

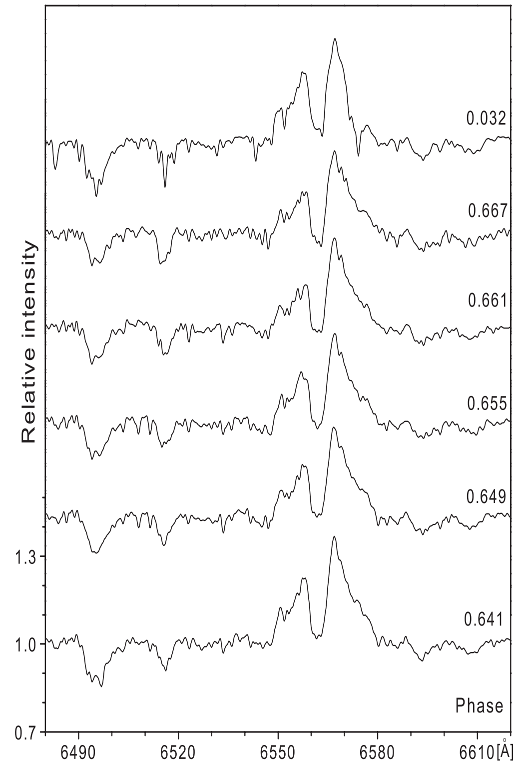

Fig. 1. The spectra of FK Com from July 3 and 4, 2002.

Table 1. Journal of observations.

Year	Month	Date	Mean S/N	Phase range	Seeing
2002	July	3	100	0.64−0.67	5
2002	July	4	100	0.032	5
2003	May	8	250	0.82−0.96	3
2003	May	9	250	0.24−0.38	3
2003	May	10	250	0.65−0.79	3
2003	May	11	250	0.14−0.21	3
2003	May	12	250	0.49	3
2003	July	20	130	0.25−0.30	6
2003	July	21	165	0.66−0.71	5
2003	July	22	115	0.09−0.12	6
2003	July	23	140	0.51−0.54	6
2004	April	29	200	0.64−0.69	3

2. Observations

We observed FK Com in the spectral range around the H_α line (6470−6670 Å) with resolution 0.19 Å/pixel during 3 years (Table 1). We used a CCD Photometrics AT200 camera with the SITe SI003AB 1024 × 1024 pixels chip mounted on the Coude spectrograph (grating B and L632/14.7°) on the 2-m telescope of the National Astronomical Observatory at Rozhen. The exposure time was 20 min. The bias frames and flat-field integrations were obtained at the beginning and at the end of each night. All stellar integrations were alternated with Th−Ar comparison source exposures for wavelength calibration.

The spectral data were reduced in a standard way using the PCIPS (Smirnov et al. 1992) and Rewia (Borkowski 1988) software packages by bias substraction, flat-field division and wavelength calibration.

The data were phased according to the ephemeris (Jetsu et al. 1993)

$$\mathrm{HJD} = (2\,439\,252.895 \pm 0.01) + (2.4002466 \pm 0.0000056) * E.$$

The normalized spectra of FK Com are shown in Figs. 1−11.

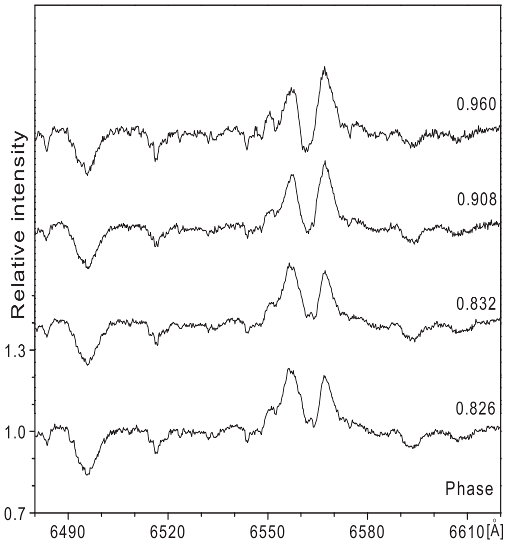

Fig. 2. The spectra of FK Com from May 8, 2003.

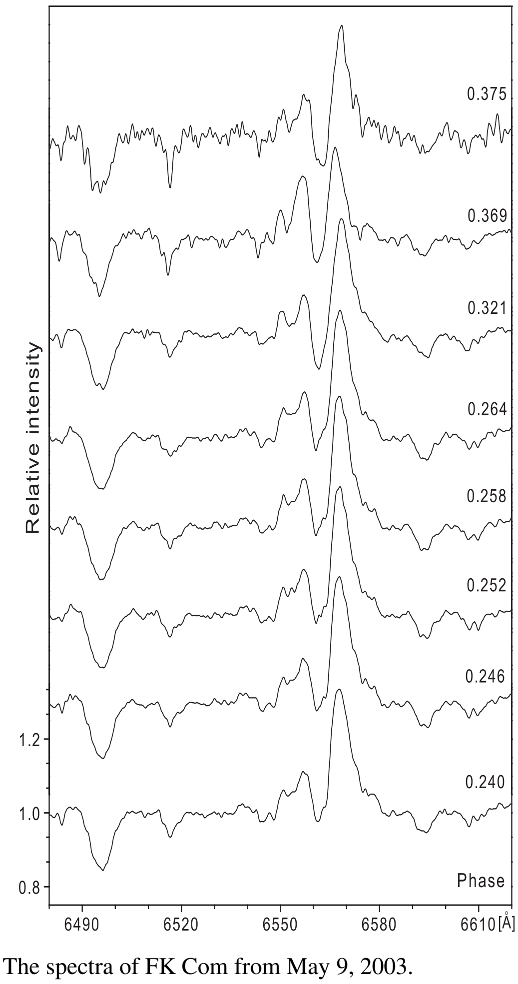

Fig. 3. The spectra of FK Com from May 9, 2003.

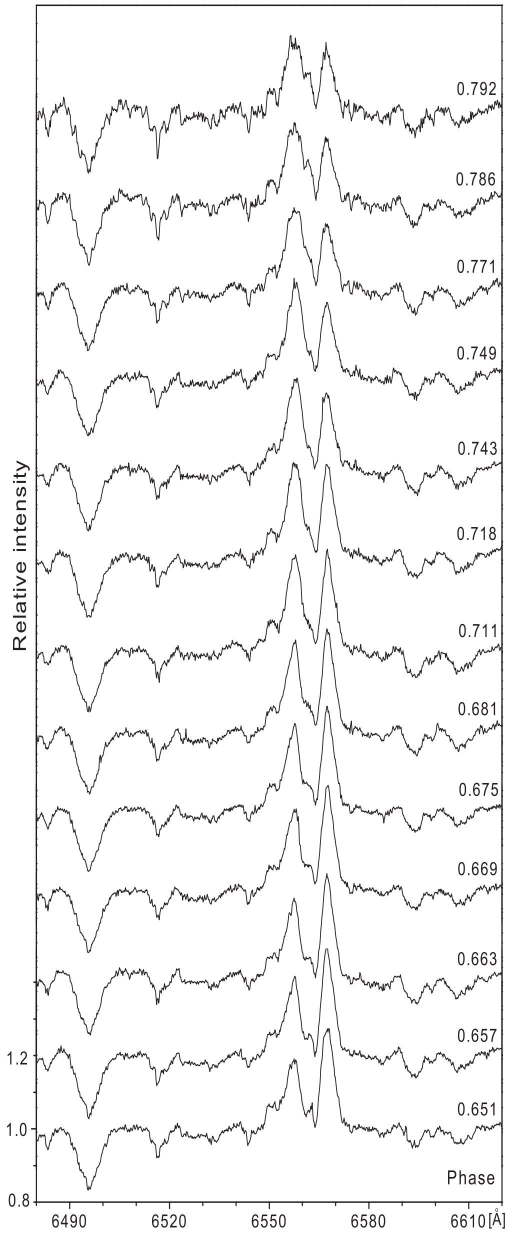

Fig. 4. The spectra of FK Com from May 10, 2003.

3. Analysis of the spectra

The analysis of the orbital variability of the spectra yields information about the dominant sources of the spectral lines as well as the locations of the active regions on star surfaces.

3.1. Variability of the H_α line

The H_α line is a spectroscopic indicator of chromospheric activity (Zarro & Rogers 1983; Herbig 1985; Frasca & Catalano 1994; Strassmeier et al. 1990) which emission excess in the active stars may appear as an emission line above the continuum or as a weak absorption line with filled-in core.

The emission H_α profile of FK Com is extremely broad, two-peaked and variable (Figs. 1–11). The two main emission peaks are at 6567.5 Å (red peak) and at 6557.5 Å (violet peak). Their intensities R and V above the local continuum (level 1) as well as their ratio V/R are introduced as measures of the variations of the H_α line.

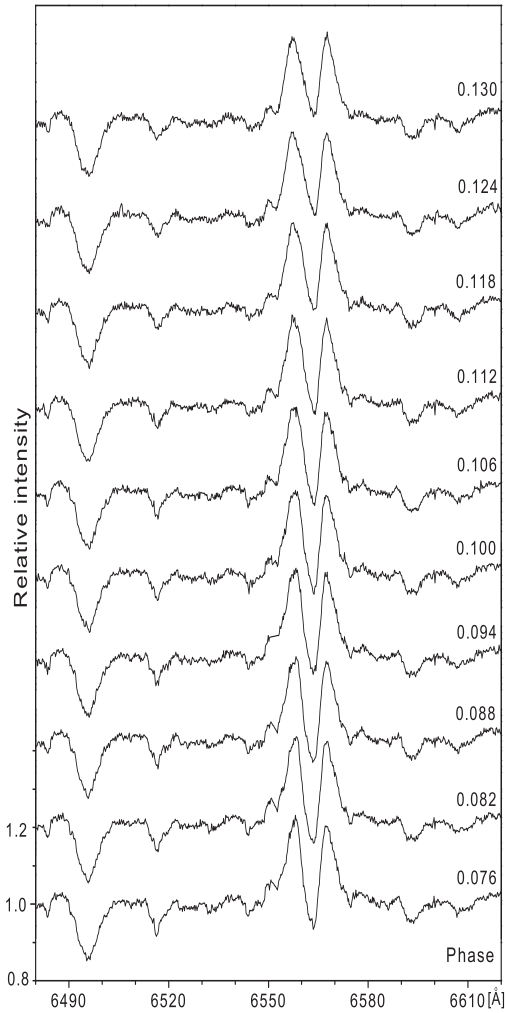

Fig. 5. The spectra of FK Com from May 11, 2003.

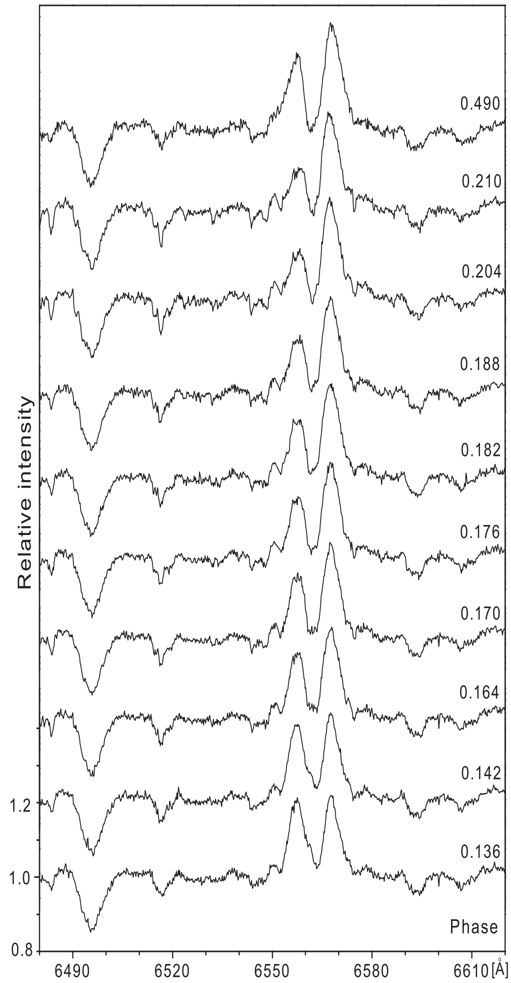

Fig. 6. The spectra of FK Com from May 11 and 12, 2003.

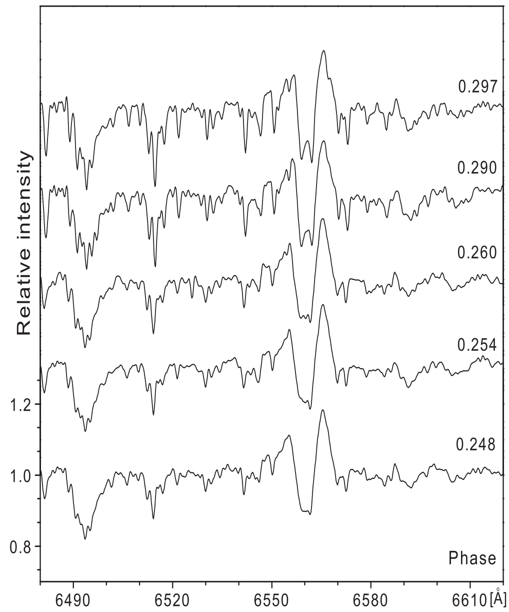

Fig. 7. The spectra of FK Com from July 20, 2003.

3.1.1. The variability of the V and R emission peaks

The width, intensity and shape of the two emission peaks of the H_α line change during the cycle:

(1) the widths of the emission peaks are nearly equal ($FWHM$ = 6 Å) at most phases. At the remaining phases there is a trend their widths to change conversely, i.e. when one of the peaks is wider the other peak to be narrower;

(2) the R peak is sharp at all phases while the V peak is smooth, with fine features at some phases (Figs. 2, 4, 6, 8 and 9);

(3) there is a third emission feature (at 6551 Å) on the left wing of the V peak that is well apparent at all phases. Similar emission feature is visible on the right wing of the R peak (6573 Å) but is considerably weaker at most phases;

(4) the V peak is slightly higher than R in the phase range 0.07−0.136 (Fig. 5). It gradually decreases during this interval while the R peak increases. The intensities of the V and R peak become equal at phase 0.13;

(5) the V peak decreases while the R peak increases in the phase range 0.13−0.21 (Fig. 6). The intensity of the R peak reaches maximum while the V peak reaches minimum at phase 0.252 (Fig. 3);

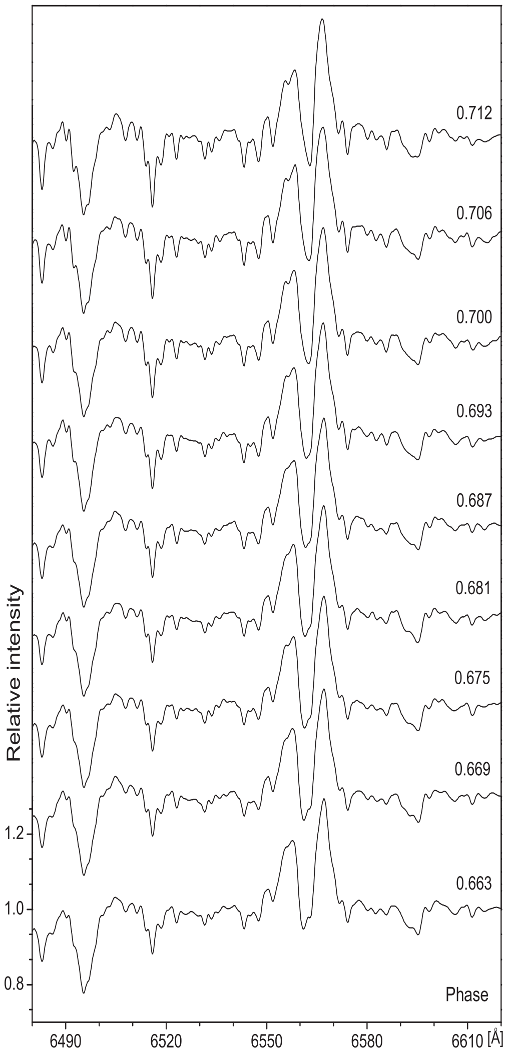

Fig. 8. The spectra of FK Com from July 21, 2003.

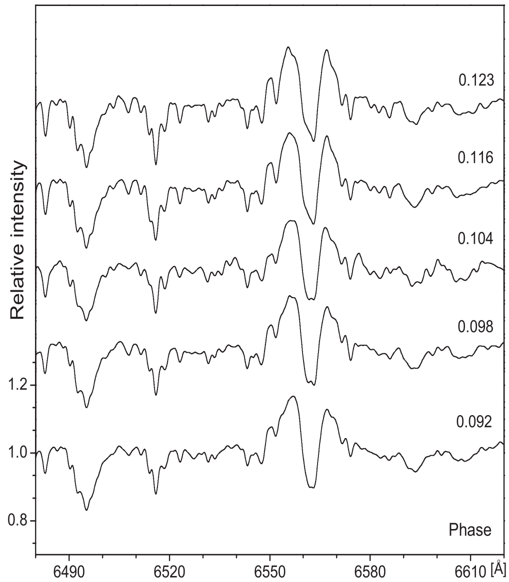

Fig. 9. The spectra of FK Com from July 22, 2003.

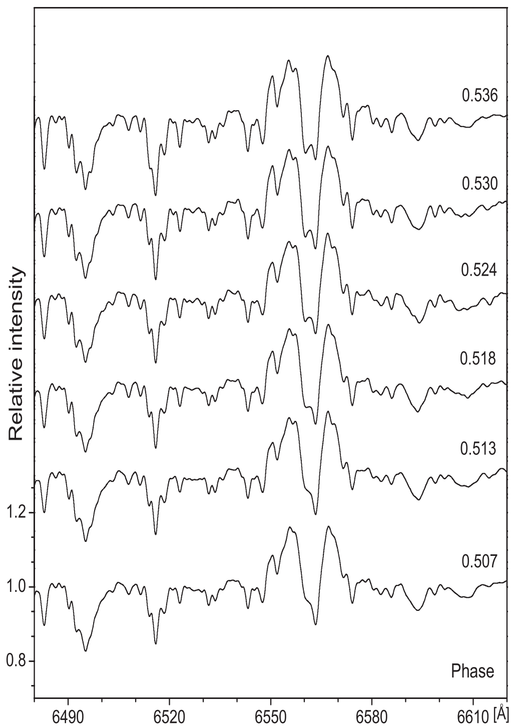

Fig. 10. The spectra of FK Com from July 23, 2003.

(6) the profiles of the H_α line are almost the same in the phase range 0.24−0.375 (Fig. 3);

(7) probably the V peak increases in the phase range 0.375−0.49 (we have no spectra in this interval) because its intensity at phase 0.49 is bigger than that at phase 0.375 (Figs. 3 and 6);

(8) the intensities of the V and R peaks are almost equal at phase range 0.507−0.536 (Fig. 10);

(9) the profiles of the H_α line are almost the same in the phase range 0.66−0.71 (Fig. 8) in which the R peak is stronger than V peak. Hence, the R peak increases while V peak decreases in the phase range 0.536−0,66 (we have no spectra in this interval);

(10) the intensities of the two emission peaks become equal at phase 0.718 (Fig. 4). The V peak is stronger than the R peak in the phase range 0.74−0.83 (Figs. 4 and 2) and reaches maximum intensity (0.32 above the continuum level) at phase 0.749 (Fig. 4);

(11) the R peak is slightly stronger than V at phases 0.908−1.03 (Figs. 1 and 2). Probably the V and R peaks become equal between phases 0.83 and 0.908 (we have no spectra in this range).

The *FWHM* of the H_α line (without the smaller bluest and reddest emission peaks) is around 17 Å and corresponds to $V \sin i = 387$ km s^{-1}. This value is close to 400 km s^{-1} determined by Walter & Basri (1982).

3.1.2. The variability of the absorption reversal

It is difficult to measure the precise λ position of the wide absorption reversal due to its asymmetry at most phases. But it seems that the position of the central absorption trends to be at

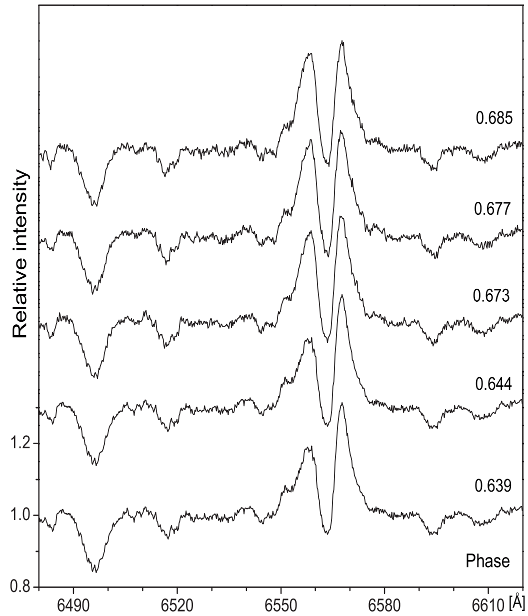

Fig. 11. The spectra of FK Com from April 29, 2004.

the H_α rest wavelength. This supports the conclusion of Walter & Basri (1982).

The mean width of the absorption reversal of the H_α line at level 1.1 (the continuum level is 1) is around 5.5 Å. This is almost the same as those of the two main emission peaks. Its shape and depth changes during the cycle:

(1) the bottom of the absorption reversal is sharp at phases 0.076−0.13 (Fig. 5) but smooth (almost flat) at phases 0.64−0.65 (Fig. 1), 0.164−0.17 (Fig. 6) and 0.248 (Fig. 7);
(2) the absorption reversal has an emission core at some phases (see phase 0.82 in Fig. 2, phase 0.65 in Fig. 4, phase 0.29 in Fig. 7 and phase 0.53 in Fig. 10);
(3) the absorption reversal is asymmetric at most phases. Its right wing is steeper than the left one at phases 0.66−0.79 (Fig. 4) and 0.076−0.13 (Figs. 5 and 9). In contrast, its left wing is steeper than the right one at phases 0.49 (Fig. 6), 0.96 (Fig. 2) and 0.32−0.37 (Fig. 3);
(4) the bottom of the absorption reversal dips below the continuum level in the phase range 0.07−0.136 (Fig. 5). Its depth begins to decrease after phase 0.106 and the bottom reaches the continuum at phase 0.124. The bottom of the absorption reversal is slightly above the continuum in the phase range 0.136−0.18 (Fig. 6). It dips below the continuum level at phases 0.32−0.375 (Fig. 3). The bottom of the absorption reversal is nearly at the continuum level at phase 0.49 (Fig. 6) as well as in the phase range 0.65−0.91 (Figs. 1, 2, 4 and 8). It is below the continuum level at phase 0.96.

3.1.3. Phase variability

Figure 12 shows the H_α profile of FK Com at some characteristic phases and illustrates the main trends of its variability.

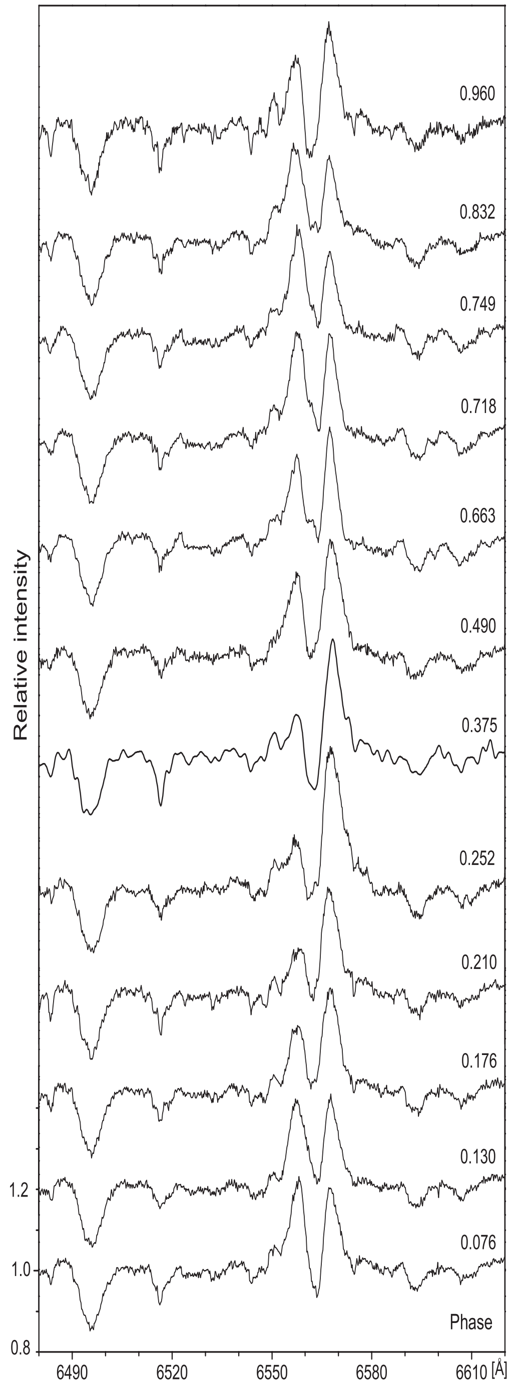

Fig. 12. Representative spectra of FK Com.

Almost all features of the H_α profile repeat at the same phases during the different observational seasons (see spectra in phases 0.64−0.68 in Figs. 1, 4, 8 and 11; spectra around phase 0.25 in Figs. 3, 6 and 7; spectra around phase 0.1 in Figs. 1, 5 and 9). This means that there is a stable phase-dependent variability of the H_α line.

We noted only two deviations from the repeatability: (a) the spectra from July 2003 differ from those in the rest of the observational seasons at the same phases by the smaller intensities of the two emission peaks and the deeper absorption reversal (compare Fig. 7 with Fig. 3; Fig. 9 with Fig. 5 and Fig. 10 with

Fig. 6). We attribute these differences to the lower quality of the spectra from July 2003 when the superposed tellurics (result of higher atmospheric humidity) cause a decrease of the emission peaks. That is why we excluded some of the July 2003 spectra (with poorest S/N) from the next analysis; (b) the absorption reversal around phase 0.65 is narrower in 2002 than in 2003 and its bottom is smooth in 2002 but is filled-in by emission in 2003 (compare Fig. 1 with Fig. 4).

It should be noted that there is not general agreement about the phase variability of the H_α line of FK Com. According to Walter & Basri (1982) the ratio V/R shows a strong phase dependence. Huenemoerder et al. (1993) find that the spectral-phase image of the subtracted H_α profiles reveals quasi-sinusoidal variation with the photometric period. However Dorren et al. (1984) do not find modulation of the H_α emission with the 2.4-day photometric period. Nations et al. (1988) conclude that its behavior varies drastically from season to season: at times there is excellent correlation of V/R with phase while the EW of H_α is almost constant; in other seasons the reverse holds; sometimes there is a weak correlation with phase for both indicators. Welty et al. (1993) concluded that during most years the V/R ratio varies regularly with the period of the light curve. Hence, the type of the modulation of the H_α emission of FK Com is not well established so far.

In order to visualize the phase variability of the main features of the H_α line as well as to check their repeatability in the different observational seasons we averaged our spectra in phase bins of 0.1 period. The phase bins, where the shape of the H_α profile changes rapidly and the phase averaging smooths this variability, were devided in two parts. Figure 13 presents the phase averaged spectra as well as the mean spectrum (averaged from all our spectra).

The phase variability of the V and R peaks, their sum $V+R$, their ratio V/R and the level of the bottom of the absorption reversal A of the H_α line of the phase averaged spectra are shown in Fig. 14.

The following trends of variability of the main H_α features could be noted (Fig. 14):

(1) the intensity of the V peak shows almost quasi-sinusoidal variability excluding the phase range around phase 0.0. It has a maximum at phase 0.75 and a minimum at phase 0.25. The amplitude of variability is 0.15. The rapid change around phase 0.0 leads to the appearance of a secondary (smaller) minimum and maximum of V before and after phase 0.0 respectively;
(2) the intensity of the R peak has a sharp maximum at phase 0.25 and minimum at phase 0.75 but does not decrease gradually between these phases. The amplitude of its variability is 0.13. The intensity of the R peak also changes rapidly around phase 0.0 but in opposite direction of the V peak. Although the course of the intensity of the R peak is complicated, it is visible that its changes are almost in anti-phase to those of the V peak;
(3) the phase variability of the ratio V/R strongly resembles that of the V emission peak;

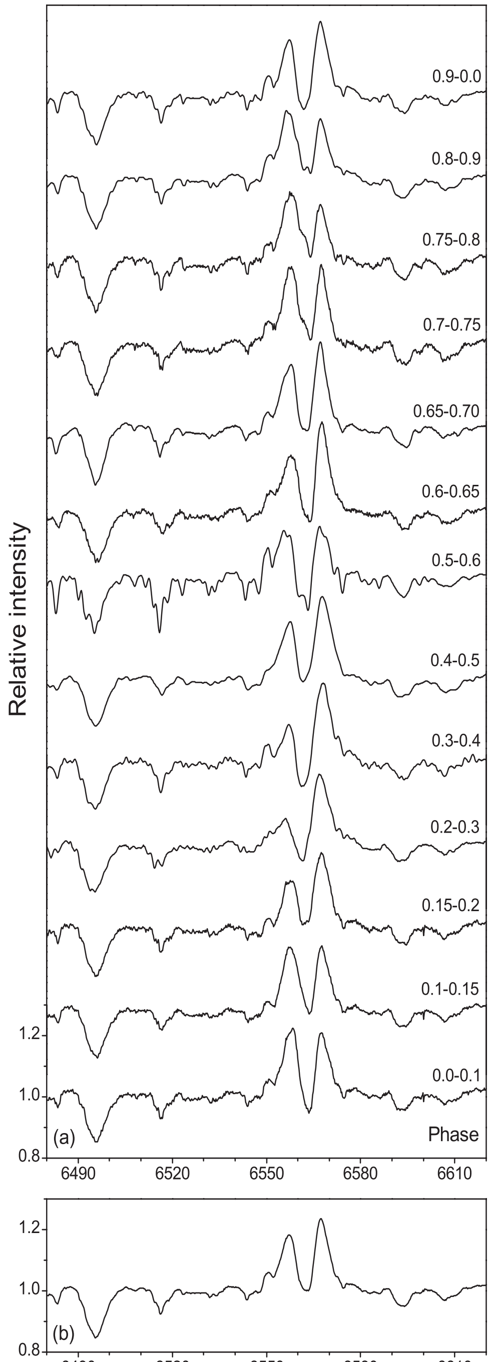

Fig. 13. a) The spectra of FK Com averaged in phase bins; **b)** the mean spectrum.

(4) the level of the bottom of the absorption reversal A is around continuum (level 1) at most phases and dips below it around phases 0.0 and 0.3;
(5) due to the almost equal widths of the two emission peaks at most phases we consider the sum of their intensities $V+R$ as a good measure of the total H_α emission. The sum $V+R$ is near to its average value (around 2.42) at most phases (Fig. 14). It has a sharp maximum at phase 0.75 and minimum at phase 0.35. The amplitude of variability of $V+R$ is 0.15. The EW of the total emission excess ranges

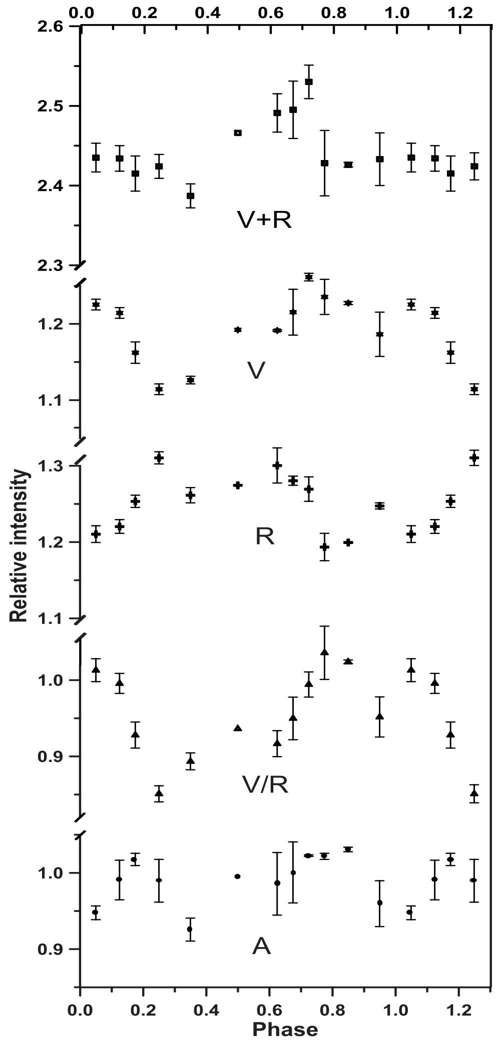

Fig. 14. The phase variability of the intensities of the *V* and *R* emission peaks, their sum $V + R$, their ratio V/R and the level of the bottom of the absorption reversal A of the H_α line. The error bars are a measure of the repeatability as well as of the rapidity of variability.

from 2.2 to 4.75 Å. Its mean value of 3.45 Å is close to the value of 3.3 Å determined by Walter & Basri (1982).

Our spectra definitely show that the *V* peak is strongest at phase 0.75 while the *R* peak is strongest at phase 0.25. This conclusion differs from those of the previous analyses: Walter & Basri (1982) established that the *V* peak is stronger around phase 0.25 and the *R* peak is stronger at phase 0.75; Ramsey et al. (1981) found that *V* is bigger than *R* in the phase range 0.1−0.55 while *R* is bigger than *V* in the phase range 0.55−1.05. There is no information about the ephemeris used by these authors but we suppose that this is the ephemeris of Chugainov (1976). The difference between the phases of our observations calculated by the ephemeris of Chugainov and that of Jetsu et al. (1993) is only +0.03. Hence, the foregoing discrepancies cannot be attributed to the different ephemeris.

3.2. Other lines in the spectra

The line 6496 Å is the second strongest line of FK Com in the observed spectral range 6470−6670 Å. It has symmetric shape with constant depth, width and λ position. This line has a *FWHM* around 7 Å and rotational broadening of about 4.2 Å (determined by fitting the central parts of the profiles with 6th-order polynomials and measuring the half width of these fits at the continuum level, Kjurkchieva et al. 2002) corresponding to $V \sin i = 191$ km s^{-1}. Probably this is a chromospheric line and belongs to CaI.

The rotational broadenings of the FeI (photospheric) lines 6517, 6594 and 6609 Å correspond to $V \sin i$ = 141 km s^{-1}. This value is in the middle of the range of previous estimations: 120 km s^{-1} (Bopp & Stencel 1981); 160±10 km s^{-1} (Eaton 1990); 200 km s^{-1} (Walter et al. 1984); 162.5 ± 3.5 km s^{-1} (Huenemoerder et al. 1993).

The different width of the spectral lines of FK Com means that they originate from different layers of the stellar atmosphere.

It should be noted that the typical values of rotation rate from G-type stars are ≤10 km s^{-1} for single stars and 30−50 km s^{-1} for stars in close binary systems. The extreme rotational velocity of FK Com raises questions about its configuration and evolutionary status.

4. Present models of FK Com

The model of the star FK Com should answer the important question about the source of its unusual H_α line. The different answers to this question lead to two types of models: a single fast-rotating star and a double system with a very low-mass secondary.

4.1. Single star

The main argument for this model is the lack of radial velocity variations of the spectral lines.

Chugainov (1977) interpret the unusual broad H_α profile of FK Com by a co-rotating, magnetically coupled envelope which is 5−10 times larger than the stellar radius.

According to Ramsey et al. (1981) FK Com is a single star formed from a recently coalesced binary system that has an asymmetric excretion disk. They attributed the changes of the V/R ratio and the broad H_α profiles to a disk (co-rotating with the star) with a substantial density inhomogeneity. A magnetic field imbedded in the disk in the form of a loop structure supports the density inhomogeneity. The material is ejected along the magnetic field lines in the loop structures as well as by large flares. Huenemoerder et al. (1993) also concluded that the Balmer emission of FK Com arises in structures similar to solar prominences.

Welty et al. (1993) suppose that there must be a localized emission region on/or above the stellar surface in addition to more distributed emission on the stellar surface or from the near circumstellar environment or both. The double-peaked H_α profile is considered as an indicator of a circumstellar disk. The quasi-sinusoidal variation of the radial velocity of the dominant component of the residual H_α emission is explained by a localized emitting region (emitting blob). The weak emission excess during the transition from being most blue-shifted to being most red-shifted is explained by occultation of the star by emitting material. The variations of the widths of the photospheric lines are attributed to occultations of different regions of the visible photosphere by the orbiting blob. Such a blob would occult the star for a small part of the cycle that is inconsistent with the observed nearly sinusoidal photometric variability.

Oliveira & Foing (1999) model the asymmetric Balmer lines by 3 co-rotating, emitting structures corresponding to different distances from the rotational axis and longitudes. The *V* and *R* changes are attributed to density inhomogeneity corotating with the star.

Korhonen et al. (2000) interpreted their observations with a model of constant emission from the chromosphere, seen during the minimum of the emission and matter flowing up from the active region and resulting in variable rotationally modulated emission. When the spots are at the center of the disk the flow is strongest and towards the observer, so the largest emission is in the blue wing. Half a rotation later the flow is pointed away and the strongest emission is in the red wing. This model suggests hot active plages in the chromosphere in the vicinity of the spots with outflows of about 200 km s^{-1}.

Welty & Ramsey (1994a) attributed the variations of $V \sin i$ of FK Com to changes of the star shape of the order of 2.5% due to strong non-radial pulsations excited by a recent binary merger.

The single-star models suppose that FK Com is evolved from a close binary, perhaps by coalescence of a W UMa system. Webbink (1976) suggests that when the former binary system dissipates its angular momentum during mass loss an excretion disk may form. The rapid rotation would arise from the angular momentum of the former binary and the activity from a rotation-driven magnetic dynamo (Ramsey et al. 1981).

4.2. Double system

The long-term stability of the brightness and H_α variations is one of the main arguments for the binary model (Rucinski 1991) since dark spots appearing always at the same longitudes seem improbable.

Walter & Basri (1982) assumed that the 2.4 day stellar rotation is identical to the orbital period of the binary in which the low-mass component ($q \leq 0.09$) loses mass through Roche lobe overflow. The accretion disk cannot form due to the size of the primary but the accreting gas causes a shock in the G giant atmosphere. The accreted material forms a warm extended halo that occupies that region of the stellar atmosphere not occupied by closed magnetic flux tubes. The photosphere is back heated by the warm halo producing the visual light variations. The central absorption feature of the H_α line is attributed to the star photosphere or contribution from cool material in orbit outside the accretion stream. The H_α emission originates in the warm halo due to the recombination of the hydrogen ionized by the impact of accreting gas.

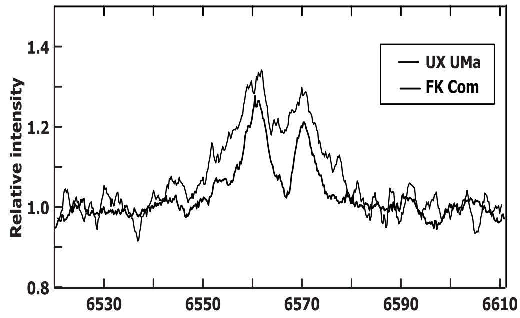

Fig. 15. The similarity of the H_α lines of FK Com and UX UMa at the same phase 0.75.

Walter & Basri (1982) argued that the bright hemisphere of FK Com is an accretion-induced phenomenon unrelated to the "normal" chromospheric and coronal activity generated by the rapid stellar rotation both in RS CVn- and BY Dra-type stars. The photometric behavior of FK Com is attributed to a hot photospheric spot below the H_α emitting region. If the inclination is $i \leq 90°$ and the distance of the H_α emitting region from the stellar surface is sufficiently large, then it is visible at all phases and no strong variation of the total H_α emission is expected. But extra polarization should be detected (due to the scattering) when the H_α region is near the stellar limb (at phases 0.25 and 0.75). Huovelin et al. (1987) do find variable wavelength-dependent polarization of the emission of FK Com.

According to the binary model at the present epoch FK Com has a large mass ratio making it to look like a single rapidly rotating giant and it is the best example of the short-lived final stage in the death of very close binary system. The low-mass secondary of FK Com is likely to be close to becoming a naked stellar core and the primary is ascending to the giant branch. In the past FK Com could have been either an Algol system or an RS CVn binary (Walter & Basri 1982).

5. Our model of the H_α emitting configuration of FK Com

The observed H_α profile of FK Com is not similar to those of the RS CVn stars. Some of this type stars show also H_α lines in emission but they are single-peaked. In contrast, the double-peaked H_α line of FK Com is very similar in shape to that of the nova-like cataclysmic star UX UMa (Fig. 15) that we observed with the same equipment (Marchev & Kjurkchieva 2003).

The similarity of the H_α line of FK Com to that of UX UMa appears also in: (a) almost equal intensities of the emission peaks above the continuum level; (b) almost equal widths of the absorption reversal, the two emission peaks as well as the whole H_α profile; (c) the variable depth of the absorption reversal during the cycle; (d) the presence of additional emission features on the blue wing of the *V* peak as well as on the red wing of the *R* peak; (e) the same ratio V/R at phase 0.75.

We also found a similarity of the H_α line of FK Com with (a) the shape and phase variability of the H_β and H_γ lines of the cataclysmic SU UMa-type star HT Cas (Catalan 1995); (b) the H_α line of the T Tau-type star AA Tau (Hartmann 1998).

The present models of the nova-like cataclysmic stars (such as UX UMa), SU UMa cataclysmic stars (as HT Cas) and T Tau stars (as AA Tau) include disk structure as a source of the wide two-peaked emission Balmer lines. Then the similarity of the H_α line of FK Com to the Balmer lines of the foregoing disk-like stars suggests that the broad H_α line of FK Com originates from an extended disk.

It is reasonable to suppose that this disk is the dominant source of the H_α emission of FK Com and produces its mean asymmetric H_α profile (with unequal emission peaks). Then the variability of the H_α line may be attributed to additional source(s) of emission and/or absorption whose radial velocity and contribution changes during the cycle.

In order to visualize this variability we subtracted the mean spectrum from the phase averaged spectra. The difference spectra are shown in Fig. 16.

The averaged H_α profiles differ mostly from the mean profile at phase ranges 0.2−0.3 and 0.7−0.8. The difference spectra at these ranges have shape of mirror images and lead to the following conclusions:

(a) there is a bulk of emission at phase 0.25. This means that there is an additional source of H_α emission moving away from the observer at this phase. The wavelength of the maximum of the emission bulk is around 2 Å longer than that of the *R* peak;
(b) there is a bulk of absorption at phase 0.25 that almost coincides with the *V* peak. This means that there is an additional source of H_α absorption moving towards the observer at phase 0.25;
(c) the amplitude and the area (*EW*) of the bulk of the emission is bigger than that of the absorption at phase 0.25;
(d) the wavelength of the maximum of the absorption bulk at phase 0.75 is around 2 Å longer that that of the *R* peak. This means that the additional source of H_α absorption moves away from the observer at phase 0.75;
(e) the wavelength of the maximum of the emission bulk at phase 0.75 is 2−3 Å longer than that of the *V* peak. This means that the additional source of H_α emission moves towards the observer at phase 0.75;
(f) the amplitude and the area (*EW*) of the bulk of emission at phase 0.75 is also bigger than that of absorption.

Hence, the sources of additional emission and absorption move in opposite directions with respect to the observer at phases 0.25 and 0.75. They have maximum radial velocities at these phases (Fig. 16) and the ranges of variability of their radial velocities are almost the same. The contribution of the source of additional emission in H_α is bigger than that of additional absorption.

The repeating of the H_α line shape at phases 0.25 and 0.75 during 3 observational seasons means that the foregoing characteristics of the profile are not transient but are signs of reliable inherent structures.

The amplitude and area (*EW*) both of the bulk of emission and absorption at the remaining phases are smaller than those at phases 0.25 and 0.75. The shapes of the difference spectra at these phases are not as simple as those at phases 0.25 and 0.75.

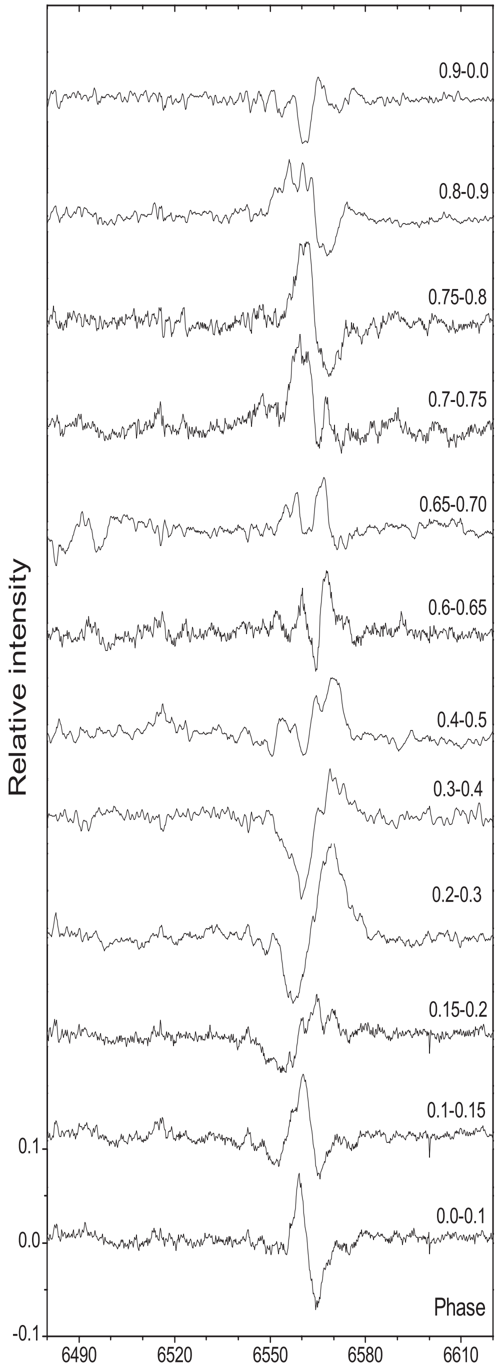

Fig. 16. The differences between the spectra averaged in phase bins and the mean spectrum.

Most of the difference spectra have more features in the H_α region compared with the quasi-sinusoidal shapes of this range at phases 0.25 and 0.75. However, the most smoothed difference spectra also show a quasi-sinusoidal shape of the H_α region. We measured the wavelengths of the maxima of the bulk of emission and absorption at the phases at which they are well apparent. These values were used for calculation of the radial velocities of the source of additional emission (SAE) and absorption (SAA). Figure 17 presents the phase variations of these radial velocities.

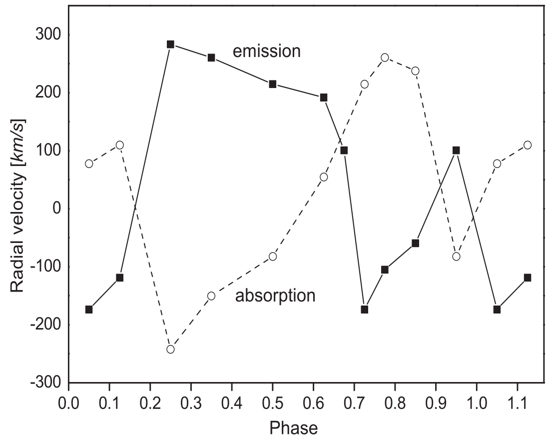

Fig. 17. Radial velocities of the sources of additional H_α emission and absorption during the cycle.

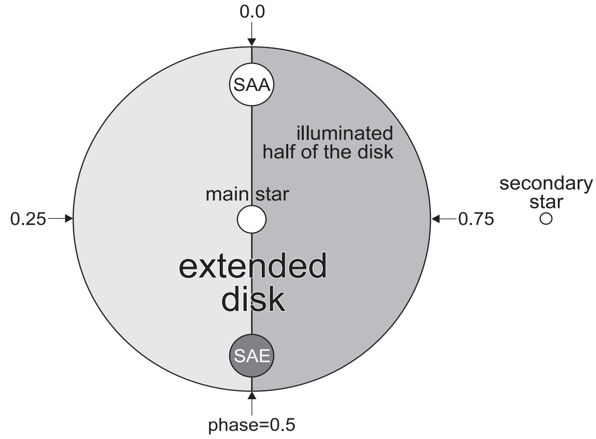

Fig. 18. The H_α emitting configuration of FK Com according to our spectra: main star (source of the absorption reversal); extended disk (source of the two-peaked emission line); SAE (Source of the Additional Emission); SAA (Source of the Additional Absorption); secondary star (source of the illumination of the disk).
Note: The color intensity at a given point is proportional to the its H_α emissivity; the arrows are along the observer's direction at the main phases; the scales of the structures are arbitrary.

A trend is visible the radial velocities of SAA and SAE to change in anti-phase. The two radial velocity curves consist of two main parts. The first part has a slightly larger amplitude and longer duration than the second one. Moreover, similarly to the intensities of the *R* and *V* peak (Fig. 13), there is a rapid change of the radial velocities of SSA and SAE around phase 0. The shape of the radial velocity curves in Fig. 17 resembles that of the object SS 433 with a precessing accretion disk.

Due to the almost equal widths of the two emission peaks of the H_α line during most of the cycle we assume that it is less probable that the inequality of the *R* and *V* peak of the mean H_α profile is caused by some considerable geometric asymmetry of the disk. It rather may due to inhomogeneous H_α emissivity of the disk surface. This inhomogeneity is long-lived because the mean H_α profile remains the same during the three years of our observations. It may be attributed to a different density and/or temperature of the regions of the disk that produce the two emission peaks. Such an inhomogeneity may be explained as a result of illumination of half a disk. A hot (accretion) spot on the surface of the central star cannot produce the needed illumination because a source inside the disk would not be able to light half of its surface. It is reasonable to assume that the source of disk illumination is a hot object synchronously orbiting the disk (similar to the naked stellar core proposed by Walter & Basri 1982). This supposition leads in turn to a binary configuration of FK Com.

The anti-phase motion of SAE and SAA as well as the equal ranges of changes of their radial velocities means that these additional sources are at diametrically opposite regions of the rotating disk surface. Moreover, the values of the maximum radial velocities of SAE and SAA lead to the conclusion that their distances from the disk center are near to the distances of maximum H_α emissivity of the disk (producing the *V* and *R* peak). We assume that the explanation of the variable additional emission and absorption in the H_α line by obscuration of the disk by the secondary star is less probable because the star disks usually lie on the orbital planes of binaries.

The bright spot created by mass transfer in a binary system supposed by Walter & Basri (1982) may be a source of the additional H_α emission (SAE). We do not have reasonable idea about the nature of the additional source of H_α absorption (SAA).

The model of FK Com consisting of a half-illuminated disk with diametrically opposite sources of emission and absorption on its surface (Fig. 18) explains well the main phase variations of the H_α line:

(a) the contributions of the additional sources of emission and absorption compensate each other at phases 0.0 and 0.5. The higher *R* peak at phase 0.5 is explained by the positive radial velocity of the illuminated half of the disk at this phase while the lower *R* peak at phase 0.0 is explained by the negative radial velocity of the illuminated half of the disk at this phase;
(b) the highest *R* peak and the lowest *V* peak at phase 0.25 can be explained by the superposing of the contributions of the additional sources: SAE has maximum positive radial velocity while SAA has maximum negative radial velocity at this phase;
(c) the highest *V* peak and lowest *R* peak at phase 0.75 can be explained by the superposing of the contributions of the additional sources: SAE has maximum negative radial velocity while SAA has maximum positive radial velocity at this phase;
(d) the greater total H_α emission at phase 0.75 can be explained by the fact that the illuminated part of the disk is towards the observer at this phase;
(e) the rapid changes of the H_α profile around phase 0.0 (Fig. 14) might be attributed to the consecutive superposing of the contributions of the source of additional absorption, the main star and the source of additional emission.

So, the analysis of our spectra allows us to propose a model of the H_α emitting configuration of FK Com consisting of a main star that is a source of the absorption reversal of the H_α line; an extended disk around the main star that is a source of the dominant component of H_α emission; a secondary hot object that illuminates the disk; additional sources of emission and absorption at diametrically opposite regions of the disk.

The disks are considered as a result of accretion in binary systems. Their main appearances are broad two-peaked emission lines. These are typical features of cataclysmic variables and are attributed to stable Keplerian disks. The long-period Algol-systems ($P > 6$ days) also display strong double-peaked H_α emission lines indicating the presence of a classical accretion disk. The short-period Algols ($P < 6$ days) show weak transient H_α emission. It is supposed that the stable disks of the long-period Algol systems may form due to the small size of their primaries relative to the binary separation. In contrast due to the large size of the primaries of the short-period Algols the high velocity gas stream forms circum-primary distribution of gas (accretion annulus) or quasi-stable accretion disks. The Doppler tomography of the H_α spectra of Algol itself shows several sources of emission (from strongest to weakest): a gas stream, a localized turbulent region of gas just above the photosphere of the primary and an accretion annulus (Richards et al. 1996).

The main characteristics of the observed H_α line of FK Com remain constant during a long period. The shape of its profile is the same as those of cataclysmic stars and long-period Algols. This leads us to the supposition that FK Com has a stable accretion disk.

6. Conclusion

The main results of our H_α observations of FK Com can be summarized as follows:

(1) The average intensity of the R peak is bigger than that of the V peak.
(2) The intensities of the V and R emission peaks change almost in anti-phase.
(3) The ratio V/R varies in phase with V.
(4) The total H_α emission has a maximum around phase 0.75.
(5) There is a rapid variability of the intensities of two emission peaks around phases 0.0.
(6) On the basis of the similarity of the H_α profile of FK Com and those of the disk-like cataclysmic stars we concluded that the dominant source of the broad two-peaked H_α line of FK Com is an extended disk. The asymmetry of the mean H_α profile requires the disk to be half-illuminated. This leads in turn to the conclusion that FK Com is a binary star.
(7) The variability of the H_α profile is attributed to additional sources of emission and absorption. The radial velocities of these sources change in anti-phase.

As a result of the analysis of our spectral observations we propose a model of the H_α emitting configuration of FK Com consisting of a main star; a half-illuminated disk; sources of additional emission and absorption at diametrically opposite regions of the disk; a low-mass hot secondary object.

Acknowledgements. The authors are grateful to the anonymous referee for very useful remarks and suggestions which allowed us significantly to improve this paper. The research was supported partly by funds of project F1411/2004 of the Bulgarian Ministry of Education and Science as well as project No. 19/2004 of Shumen University.

References

Bianchi, L., Grewing, M., & Kappelmann, N. 1985, A&A, 149, 41
Bianchi, L., & Grewing, M. 1987, in Circumstellar Matter, ed. I. Appenzeller, & C. Jordan, 363
Bidelman, W. 1954, ApJS, 1, 175
Bolton, T. 1978, in a circular of the RS CVn Working Group of the IAU Commission, ed. D. S. Hall, 42
Bopp, B., & Evans, D. 1973, MNRAS, 164, 343
Bopp, B., & Stencel, R. 1981, ApJ, 247, L131
Bopp, B., & Rucinski, S. 1981, in Fundamental Problems in the Theory of Stellar Evolution, ed. D. Sugimoto, D. Schramm, & D. Lamb (Dordrecht: Reidel), IAU Symp., 93
Bopp, B. 1982, in Proc. Second Cambridge Workshop on Cool Stars, Stellar Systems and the Sun, SAO Special Report, No. 392, 1, 207
Borkowski, G. 1988, Internal report of Astron. Inst. in Torun, Poland
Carniero, J. 1990, A&SS, 169, 101
Catalan, M. 1995, Ph.D. Thesis, The University of Sussex
Chugainov, P. 1966, IBVS, No. 172
Chugainov, P. 1976, Izv. Krymsk. Astrofiz. Obs., 54, 89
Chugainov, P. 1977, Izv. Krymsk. Astrofiz. Obs., 57, 31
Cutispoto, G., Pagano, I., & Rodono, M. 1992, A&A, 263, L3
Dorren, J., Guinan, E., & McCook, G. 1983, IBVS, No. 2276
Dorren, J., Guinan, E., & McCook, G. 1984, PASP, 96, 250
Eaton, J. 1990, IBVS, No. 3460
Eggen, O., & Iben, I. 1989, AJ, 97, 431
Jetsu, L., Pelt, J., Tuominen, I., & Nations, H. 1991, in The Sun and cool stars: activity, magnetism, dynamos, ed. I. Tuominen, D. Moss, & G. Rudiger (Heidelberg: Springer), Proc. IAU Coll., 130, 381
Jetsu, L., Anttila, R., Dimitrienko, E., et al. 1992, A&A, 262, 188
Jetsu, L., Pelt, J., & Tuominen, I. 1993, A&A, 278, 499
Jetsu, L., Tuominen, I., & Antov, A. 1994, A&AS, 103, 183
Frasca, A., Marino, C., Catalano, S., & Marilli, E. 2000, A&A, 358, 1007
Frasca, A., & Catalano, S. 1994, A&A, 284, 883
Gondoin, P., Erd, C., & Lumb, D. 2002, A&A, 383, 919
Guinan, E., & Robinson, C. 1986, AJ, 91, 935
Hall, D. 1976, in Multiple Periodic Variable Stars, ed. W. Fitch (Dordrecht: Reidel), IAU Coll., 29, 287
Hartmann, L. 1998, in Accretion Processes in Star Formation, Cambridge Astrophys. Ser., 32, 119
Herbig, G. 1958, ApJ, 128, 259
Herbig, G. 1985, ApJ, 289, 269
Huenemoerder, D., Ramsey, L., Buzasi, D., & Nations, H. 1993, ApJ, 404, 316
Hughes, V., & McLean, B. 1987, ApJ, 313, 263
Huovelin, J., Pirola, V., Vilhu, O., Efimov, Y., & Shakhovskoy, N. 1987, A&A, 176, 83
Kjurkchieva, D., Marchev, D., & Zola, S. 2002, A&A, 386, 548
Korhonen, H., Berdjugina, S., & Tuominen, I. 2002, A&A, 390, 179
Marchev, D., & Kjurkchieva, D. 2003, Collected papers Physics, ISBN 954-577-163-1, 158
McCarthy, J., & Ramsey, L. 1984, ApJ, 283, 200
Merrill, P. 1948, PASP, 60, 382
Morris, S., & Milone, E. 1983, PASP, 95, 376
Nations, H., Buzasi, D., Huenemoerder, D., & Ramsey, L. 1988, BAAS, 20, 1023

Oliveira, J., & Foing, B. 1999, A&A, 343, 213
Ramsey, L., Nations, H., & Barden, S. 1981, ApJ, 251, 101
Richards, M., Jones, R., & Swain, M. 1996, ApJ, 459, 249
Richards, M. 1992, ApJ, 387, 329
Richards, M. 1993, ApJS, 86, 255
Rucinski, S. 1981, A&A, 104, 260
Rucinski, S. 1991, AJ, 101, 2199
Smirnov, O., Piskunov, N., Afanasyev, V., & Morozov, A. 1992, in ASP Conf. Ser., 26, Astronomical Data Analysis Software and Systems, 1, 344
Strassmeier, K., Fekel, F., Bopp, B., Dempsey, R., & Henri, G. 1990, ApJS, 72, 191
Tuominen, I., Berdyugina, S., & Korpi, M. 2002, AN, 323, 367
Walter, F. 1981, ApJ, 245, 677
Walter, F., & Basri, G. 1982, ApJ, 260, 735
Walter, F., Neff, J., Bopp, B., & Stencel, R. 1984, in Proc. Third Cambridge Conf. on Cool Stars, Stellar systems and the Sun
Webbink, R. 1976, ApJ, 209, 829
Welty, A., Ramsey, L., Iyengar, M., Nations, H., & Buzani, D. 1993, PASP, 105, 1427
Welty, A., & Ramsey, L. 1993, BAAS, 25, 1458
Welty, A., & Ramsey, L. 1994a, AJ, 108, 299
Welty, A., & Ramsey, L. 1994b, ApJ, 435, 848
White, N., Shafer, R., Parmar, A., & Culhane, J. 1987, in Cool Stars, Stellar Systems, and the Sun, ed. J. Linsky, & R. Stencel (Berlin: Springer), 521
Zarro, D., & Rogers, A. 1983, ApJS, 53, 815